

# Analytical evaluation of CPTu soundings in soft Chicago clay

S. S. Agaiby

Cairo University, Giza, Egypt: shehabagaiby@cu.edu.eg

P. W. Mayne

Georgia Institute of Technology, Atlanta, GA, USA: paul.mayne@ce.gatech.edu

**ABSTRACT:** Results from piezocone tests in soft lacustrine clay at the national geotechnical experimentation site (NGES) at Northwestern University are used to interpret effective friction angle, rigidity index, undrained shear strength, and yield stress ratio (YSR) with depth. The effective friction angle is evaluated using an effective stress limit plasticity solution derived by the Norwegian Institute of Technology (NTH). A hybrid spherical cavity expansion – critical state soil mechanics (SCE-CSSM) framework provides the undrained rigidity index ( $I_R$ ) based on cone tip resistance and porewater pressure readings. The evaluated  $I_R$  is utilized in evaluating three separate formulations for YSR from SCE-CSSM in terms of net cone resistance, excess porewater pressure, and effective cone resistance. These three profiles fully agree and match with laboratory reference values obtained from standard consolidation tests on undisturbed samples. Finally, the method gives good agreement with lab-measured undrained shear strengths from CAUC tests using the corresponding cone bearing factor obtained from the acquired value of  $I_R$ .

**Keywords:** In-situ testing; piezocone; undrained rigidity index; undrained shear strength; stress history.

## 1. Introduction

The rigidity index ( $I_R$ ) is an important input parameter for geotechnical applications involving bearing capacity, driven pile foundations, porewater pressure generation, and piezodissipations. The value of soil rigidity index is incorporated in various theories and analytical solutions involving cavity expansion, strain path method, and finite element analyses. For piezocone penetration into clays, the magnitude of undrained rigidity index is often needed in the interpretation of coefficient of consolidation ( $c_{vh}$ ) and its associated hydraulic conductivity ( $k$ ).

The rigidity index is defined as the ratio of shear modulus to shear strength,  $I_R = G/\tau_{max}$ . The value of rigidity index depends on the conditions of loading, and for undrained conditions at constant volume, the modulus and undrained shear strength can both be determined from laboratory tests such as direct simple shear or triaxial compression tests. For undrained loading, the rigidity index is given by:

$$I_R = \frac{G}{s_u} = \frac{E_u}{3 \cdot s_u} \quad (1)$$

Direct evaluation of rigidity index from its definition as the ratio of shear modulus ( $G$ ) to shear strength ( $I_R = G/s_u$ ) is quite elusive [1;2]. For one, shear modulus of any given clay can be evaluated over a wide range of mobilized strengths and levels of strain. The value of  $G$  varies and can be taken as the initial tangent shear modulus at small strains ( $G_0 = G_{max}$ ), or as either a tangent modulus ( $G_{tan} = d\tau/d\gamma_s$ ) or as a secant value ( $G_{sec} = \tau/\gamma_s$ ), as well as the value at the failure strain,  $G_f = \tau_{max}/\gamma_f$ . This is so in part because of the highly nonlinear stress-strain-strength behavior of soil, and corresponding range of stiffness that is represented in terms of modulus reduction curves, ( $G/G_{max}$ ), that decrease with increasing strain or mobilized strength [3].

Figure 1 expresses the relationship between shear stress and shear strain with a definition of the rigidity index taken at  $G_f$  or  $G_{min}$ . For penetration tests, as in the case of CPT, the appropriate value of the shear modulus is likely close to the minimum shear modulus, as defined at peak shear stress:  $G_{min} = \tau_{max} / \gamma_f$ , where  $\gamma_f$  = strain at failure [4]. As presented in Figure 1, the corresponding value for  $I_R$  can be taken as the reciprocal of the strain at failure,  $I_R = 1/\gamma_{REF}$ .

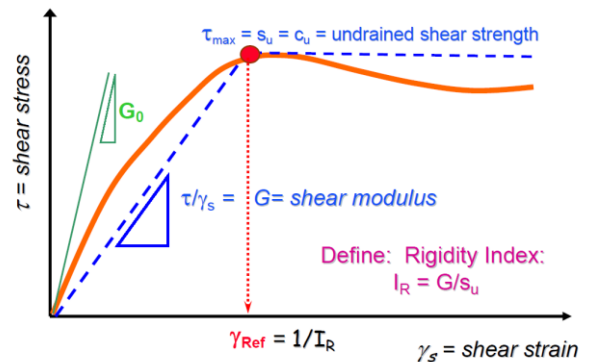


**Figure 1.** Schematic diagram illustrating shear stress vs. shear strain for clay soils and definitions of  $\tau_{max}$ ,  $G$ ,  $\gamma_f$ , and  $I_R$  [4].

## 2. Intermediate Stiffnesses of the Soil

Given the high non-linearity in the stress-strain-strength behavior of different geomaterials, it is difficult to assign a single set value of the appropriate shear modulus. As presented in Figure 1, the shear modulus definition depends on the corresponding shear strain level, since decreasing magnitudes of shear moduli are obtained at increasing shear strains. The range of the measured shear strains depends on the testing tool or technique employed, geophysical tests cover very small shear strain levels  $< 10^{-6}$  while in-situ tests such as the flat dilatometer

test (DMT) detect a higher range of about  $10^{-3}$  while penetration tests such as the CPT captures much higher shear strain levels on the order of 1% to 100%. Figure 2 presents a schematic of the shear modulus reduction with the variation in the measured shear strain level with the appropriate measuring tool for each stage.

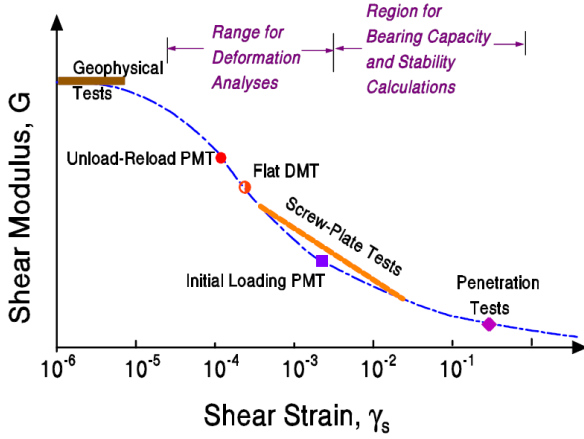


Figure 2. Reduction of shear modulus with shear strain level [5].

### 3. Undrained Rigidity Index Definition

When a cone penetrometer is pushed into the ground, a bulb of soil around the cone is deformed plastically. According to spherical cavity expansion theory, the size of the zone of the soil that goes plastic (diameter  $D$ ) is related to the size of the intruding body (diameter  $d$ ) and that ratio depends upon the rigidity index [6]:

$$D/d = (I_R)^{0.33} \quad (2)$$

Therefore, the rigidity index can be considered as a measure of the volume of clay affected by the advancing penetrometer and thus an operational value should be considered.

The main quantities defining the magnitude of the rigidity index are the shear modulus and undrained shear strength. The selection of the appropriate means to measure  $G$  and/or  $s_u$  is challenging and requires careful evaluation. In the simulation of the piezocone advancement into the ground, it is challenging to assign the predominant failure mode(s) that exist around the penetrometer. Hence, the selection of the correct shearing mode and testing technique is not straight forward. Keaveny [7] and Schnaid et al. [8] assigned the mode of  $CK_0UC$  triaxial compression, while Konrad and Law [9] recommended a pressuremeter mode. In addition, Teh and Houlsby [10] and Yu and Mitchell [11] deemed the triaxial compression mode as the most appropriate.

A more difficult issue lies in the selection of the correct shear modulus as its magnitude depends on the level of shear strain. The initial shear modulus ( $G_0 = G_{max}$ ) represents the tangent modulus at very small strains, but this applies to the nondestructive region. A secant modulus ( $G = \tau/\gamma_s$ ) represents higher strain levels with  $G$  reducing with strains [4]. As a compromise, Konrad & Law [9] and Schnaid et al. [8] chose to use a shear modulus at 50% mobilized strength ( $G_{50}$ ) to give an average response.

It is evident that there are difficulties in properly selecting the strength mode and mobilization level of shear

modulus values using laboratory-based techniques. These are affected by issues related to sample disturbance, stress relief, and the high costs of obtaining and testing quality samples. Therefore, it is of great interest and benefit to develop methods of obtaining the rigidity index based on direct CPT measurements.

### 4. Methods for Estimating Rigidity Index

Keaveny and Mitchell [12] proposed an empirical approach relating the undrained rigidity index to the over-consolidation ratio (OCR) and clay plasticity index (PI). The methodology was based on results from triaxial CAUC test data on various clays where the  $I_R$  was defined using  $G_{50} = E_{50}/3$ . The developed correlation can be expressed as:

$$I_{R50} \approx \frac{\exp\left(\frac{137 - PI}{23}\right)}{1 + \ln\left[1 + \frac{(OCR - 1)^{3.2}}{26}\right]^{0.8}} \quad (3)$$

Another means to estimate the rigidity index is via an original Cam Clay derivation which was obtained by Kulhawy and Mayne [13] based on routine soil parameters. An initial modulus was evaluated by differentiation as the strain approaches zero, then using this modulus value in a normalized form to evaluate undrained rigidity index as given by the following expression:

$$I_R = \left(\frac{2}{3}\right) \cdot M \left(\frac{1 + e_0}{C_c}\right) \cdot \ln(10) \frac{[1 + \ln(OCR)] \exp(\Lambda)}{\Lambda(1 - \Lambda) OCR^\Lambda} \quad (4)$$

where  $M = (6 \sin\phi')/(3 - \sin\phi')$  = slope of the effective frictional envelope for triaxial compression in  $q$ - $p'$  space,  $\Lambda = (1 - C_s / C_c)$  = plastic volumetric strain potential,  $C_s$  = swelling index,  $C_c$  = virgin compression index,  $e_0$  is the initial void ratio, and  $OCR = \sigma_p'/\sigma_{vo}'$ . Typically, the value of  $\Lambda \approx 0.8$  from load-unload-shear lab testing, although  $\Lambda \approx 1$  in many natural clays tested in recompression, especially at low OCRs [14].

An expression for rigidity index of clays from spherical cavity expansion theory that is dependent on the CPTu normalized porewater pressure parameter ( $B_q$ ). The  $I_R$  expression is given by [15]:

$$I_R = \exp\left[\frac{2.93 \cdot B_q}{(1 - B_q)}\right] \quad (5)$$

where  $B_q = (u_2 - u_0)/(q_t - \sigma_{vo})$ . Obtained  $I_R$  values can be restricted to the rather narrow range:  $0.50 < B_q < 0.70$  and is only relevant to soft clays.

A derivation for expressing the undrained rigidity index of clays based on CPTu was developed from the hybrid spherical cavity expansion - critical state soil mechanics framework (SCE-CSSM). The  $I_R$  expression was given as [5]:

$$I_R = \exp\left[\frac{(q_t - \sigma_{vo})}{(q_t - u_2)} \cdot \left(\frac{1.5}{M} + 2.925\right) - 2.925\right] \quad (6)$$

However, as the values of net cone resistance and effective cone resistance are often close, a line-by-line evaluation of CPTu data showed that the assessed  $I_R$  profile shows variation and scatter with depth, primarily because of the exponential format.

A recent empirical approach introduced by Krage et al. [2] using the shear wave velocity profile and net cone tip resistance from SCPTu has been developed to evaluate  $I_R$  at 50% strain level and can be determined from:

$$(I_R)_{50} = \left[ \frac{1.81 \cdot G_0}{(q_{net})^{0.75} (\sigma'_{vo})^{0.25}} \right] \quad (7)$$

With consistent units used for  $G_0$ ,  $q_{net}$ , and  $\sigma'_{vo}$  terms.

## 5. Direct CPTu Solution for Evaluating Undrained Rigidity Index

### 5.1. Original SCE-CSSM Solution

A hybrid formulation of spherical cavity expansion and critical state soil mechanics (SCE-CSSM) expresses the cone tip resistance ( $q_t$ ) and porewater pressure ( $u_2$ ) using closed-form equations as follows [16;17;4]:

$$q_t = \sigma'_{vo} + [(4/3) \cdot (\ln I_R + 1) + \pi/2 + 1] \cdot (M/2) \cdot (OCR/2)^\Lambda \cdot \sigma'_{vo} \quad (8)$$

$$u_2 = u_0 + [(2/3) \cdot (\ln I_R) \cdot (M) \cdot (OCR/2)^\Lambda \cdot \sigma'_{vo}] + [1 - (OCR/2)^\Lambda] \cdot \sigma'_{vo} \quad (9)$$

The hybrid SCE-CSSM model can be rearranged to express overconsolidation ratio (OCR) of clays in three separate formulations using net cone tip resistance ( $q_{net} = q_t - \sigma'_{vo}$ ), excess pore pressure ( $\Delta u = u_2 - u_0$ ), and effective cone resistance ( $q_E = q_t - u_2$ ):

$$OCR = 2 \cdot \left[ \frac{(2/M) \cdot (q_t - \sigma'_{vo}) / \sigma'_{vo}}{(4/3) \cdot (\ln I_R + 1) + \pi/2 + 1} \right]^{(1/\Lambda)} \quad (10)$$

$$OCR = 2 \cdot \left[ \frac{(\Delta u / \sigma'_{vo}) - 1}{(2/3) \cdot M \cdot \ln(I_R) - 1} \right]^{(1/\Lambda)} \quad (11)$$

$$OCR = 2 \cdot \left[ \frac{1}{1.95 \cdot M + 1} \left( \frac{q_t - u_2}{\sigma'_{vo}} \right) \right]^{(1/\Lambda)} \quad (12)$$

Combining equations (10) and (11), the value of the rigidity index can be obtained in terms of normalized CPTu measurements and friction parameter M:

$$I_R = \exp \left[ \frac{1.5 \cdot Q + 2.925M \cdot (U^* - 1)}{Q \cdot M - M \cdot (U^* - 1)} \right] \quad (13a)$$

$$I_R = \exp \left[ \frac{1.5 + 2.925M \cdot \left( \frac{U^* - 1}{Q} \right)}{M - M \cdot \left( \frac{U^* - 1}{Q} \right)} \right] \quad (13b)$$

where  $Q =$  normalized tip resistance  $= (q_t - \sigma'_{vo})/\sigma'_{vo}$ ;  $U^* =$  normalized porewater pressure  $= (u_2 - u_0)/\sigma'_{vo}$ .

Since the expression for  $I_R$  is an exponential form, the use of (13) in line-by-line post-processing of CPTu data unfortunately results in highly variable profiles with depth, therefore a moving average is necessary for any practical use.

A stable representation for (13) is obtained in the following format:

$$I_R = \exp \left( \frac{1.5 + 2.925 \cdot M \cdot a_x}{M \cdot (1 - a_x)} \right) \quad (14)$$

where  $a_x = (U^* - 1)/Q \approx (u_2 - \sigma'_{vo})/(q_t - \sigma'_{vo})$ . Hence,  $a_x$  can be determined as a single value for any clay deposit by taking the slope of a plot of the parameter  $(U^*-1)$  versus  $Q$ , or alternatively taken as the slope of  $(u_2 - \sigma'_{vo})$  versus  $(q_t - \sigma'_{vo})$ . Using regression analyses, slightly different slope values for  $a_q$  are obtained.

Similarly by combining equations (10) and (12), the value of the rigidity index can be alternatively obtained in terms of net and effective cone tip resistance values and friction parameter M:

$$I_R = \exp \left[ a_y \cdot \left( \frac{1.5}{M} + 2.925 \right) - 2.925 \right] \quad (15)$$

where  $a_y = (q_t - \sigma'_{vo})/(q_t - u_2)$ . The value of  $a_y$  can be determined by taking the slope of a plot of the net cone tip resistance ( $q_{net}$ ) versus effective cone resistance ( $q_E$ ).

Finally by combining equations (11) and (12), the value of the rigidity index can be alternatively obtained in terms porewater measurements and effective cone tip resistance and friction parameter M:

$$I_R = \exp \left[ a_z \cdot \left( \frac{1.5}{M} + 2.925 \right) + \frac{1.5}{M} \right] \quad (16)$$

where  $a_z = (u_2 - \sigma'_{vo})/(q_t - u_2)$ . The value of  $a_z$  can be determined by taking the slope of a plot of the net cone tip resistance ( $q_{net}$ ) versus effective cone tip resistance ( $q_E$ ).

### 5.2. Effective Friction Angle Evaluation

The derived expression for rigidity index depends on the value of the effective friction angle ( $\phi'$ ). In the event that laboratory-measured values from triaxial tests are not available, the effective friction angle can be evaluated using the NTH method. This is an effective stress limit plasticity solution for undrained penetration developed by Senneset et al. [18] as presented in Figure 3. In this method, a cone resistance number ( $N_m$ ) is defined:

$$N_m = \frac{N_q - 1}{1 + N_u \cdot B_q} = \frac{q_t - \sigma'_{vo}}{\sigma'_{vo} + a'} \quad (17)$$

where  $a' = c' \cdot \cot \phi' =$  attraction,  $c' =$  effective cohesion intercept,  $N_q = K_p \cdot \exp [(\pi - 2\beta) \cdot \tan \phi']$  is the end-bearing factor for the cone tip resistance ( $q_t$ ),  $K_p = (1 + \sin \phi')/(1 - \sin \phi')$  is the passive stress coefficient,  $\beta =$  angle of plastification ( $-20^\circ < \beta < +20^\circ$ ) which defines the size of the failure zone beneath the tip, and  $N_u = 6 \cdot \tan \phi' \cdot (1 + \tan \phi')$  is the porewater pressure bearing factor. The full solution allows for an interpretation of a paired set of Mohr-Coulomb strength parameters ( $c'$  and  $\phi'$ ) for all soil types.

For soft to firm clays, it can be adopted that  $c' = 0$ , thus the term  $N_m$  simplifies to the normalized cone resistance,  $Q = q_{net}/\sigma'_{vo}$ . Further reduction is achieved by taking the angle  $\beta = 0$  for undrained loading at constant volume and an approximate expression is given by [19]:

$$\phi' = 29.5^\circ \cdot B_q^{0.121} [0.256 + 0.336 \cdot B_q + \log Q] \quad (18)$$

which is valid for the following parameter ranges:  $20^\circ \leq \phi' \leq 45^\circ$  and  $0.1 \leq B_q \leq 1.0$  and  $OCRs < 2.5$ .

### 5.3. Undrained Shear Strength Evaluation

The operational value of rigidity index  $I_R$  can be used directly to evaluate the profile of undrained shear strength of the clay with depth since it gives the cone bearing factor ( $N_{kt}$ ). The strength is obtained from:

$$s_{uc} = \frac{q_{net}}{N_{kt}} \quad (19)$$

where spherical cavity expansion theory expresses the  $N_{kt}$  in terms of the rigidity index [6]:

$$N_{kt} = [(4/3) \cdot (\ln I_R + 1) + \pi/2 + 1] \quad (20)$$

Notably, the same input parameters ( $M$  and  $I_R$ ) can be used in (10), (11), and (12) to obtain 3 independent profiles of OCR in the clay, adopting  $\Lambda = 1$ .

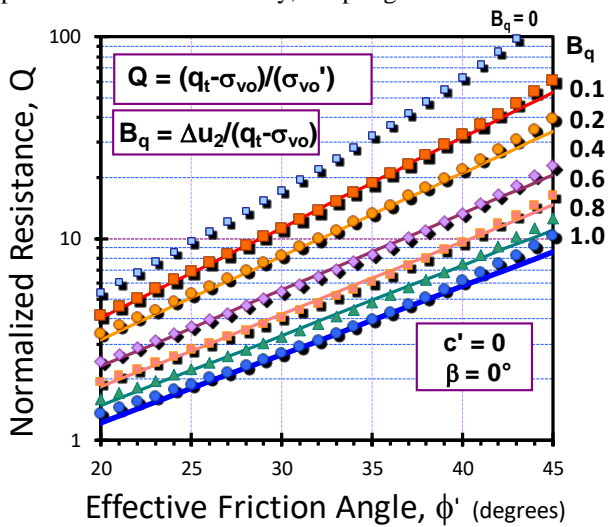


Figure 3. NTH Method for evaluating  $\phi'$  from CPTu in clays: theory shown as dots [18]; approximation by lines [4].

### 6. Case Study - soft Chicago clay, Illinois

The national geotechnical experimentation site (NGES) at Northwestern University (NWU) is in Evanston, Illinois on the northeast corner of the university campus and adjacent to Lake Michigan. The subsurface stratigraphy consists of an 8-m layer of sand overlies soft clay layers that are about 10 m to 14 m thick. The soft glaciolacustrine clays are inorganic and insensitive with mineralogy consistently predominantly of illite (55%) with lesser amounts of dolomite (18%), chlorite (9%), calcite (5%), variscite (8%), and kaolinite (4%). Index parameters of the soft Chicago clay include the following average values: natural water content  $w_n \approx 20\%$ , liquid limit  $LL \approx 38\%$ , plasticity index  $PI \approx 12\%$ , and unit weight  $\gamma_T \approx 20 \text{ kN/m}^3$  [20].

Figure 4 shows the results of a representative piezocone sounding at the site that was conducted by graduate research assistants using the Georgia Tech (GT) cone penetrometer system [21]. The CPT rig is an anchored Ford F350 flat bed truck mounted with hydraulic rams.

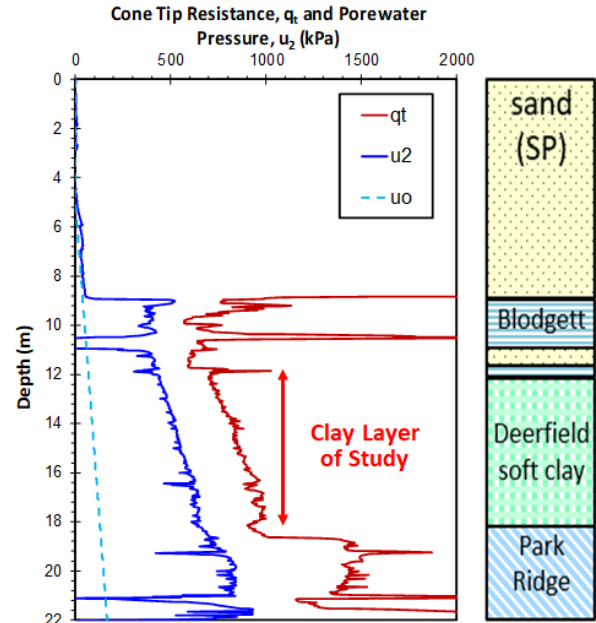


Figure 4. Piezocone sounding at NGES in Northwestern University, USA: cone tip resistance,  $q_t$ ; porewater pressure,  $u_2$  [21].

The piezocone readings were used to evaluate the normalized cone tip resistance ( $Q$ ) as the slope of  $q_{net}$  versus  $\sigma_{vo}'$  shown in Figure 5 and the normalized porewater pressure ( $B_q$ ) by plotting  $\Delta u_2$  versus  $q_{net}$  as illustrated in Figure 6 [15, 18]. The effective friction angle was evaluated using NTH method giving a value of 28.3 degrees that agrees with the friction angle from  $CK_0UC$  triaxial tests conducted by Chung and Finno [22] as shown in Figure 7.

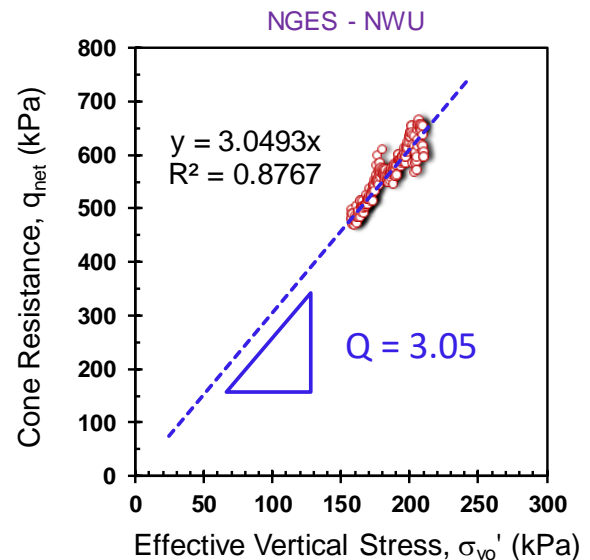


Figure 5. Evaluation of normalized cone tip resistance ( $Q$ ) using CPTu data from NGES at Northwestern, IL.

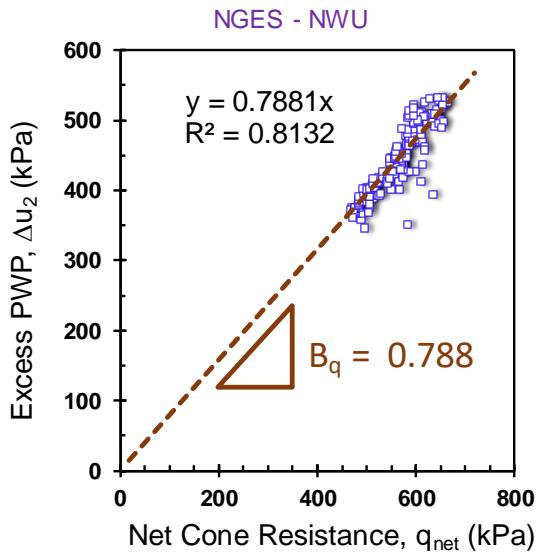


Figure 6. Evaluation of normalized porewater pressure ( $B_q$ ) using CPTu data from NGES at Northwestern University, IL

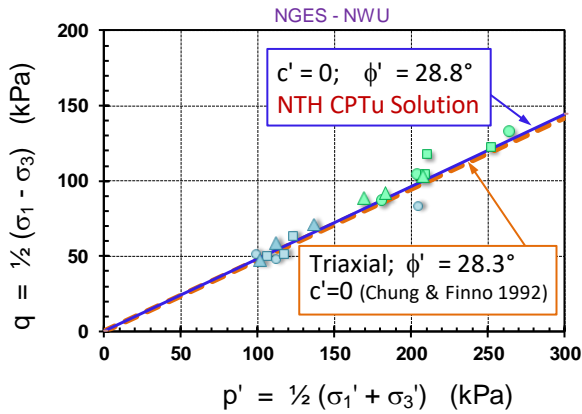


Figure 7. Comparison between NTH evaluated friction angle and laboratory measured values using CK<sub>0</sub>UC triaxial tests

Figures 8, 9, and 10 show the evaluation of the slope parameters used in the proposed  $I_R$  solution where  $\Delta u_\sigma = (u_2 - \sigma_{v0})$  is plotted versus net cone tip resistance ( $q_{net}$ ) in Figure 8, giving a slope value of  $a_x = 0.460$ . The slope value is used with the effective friction angle in Eq. (14) to give an operational rigidity index  $I_R = 147.4$ .

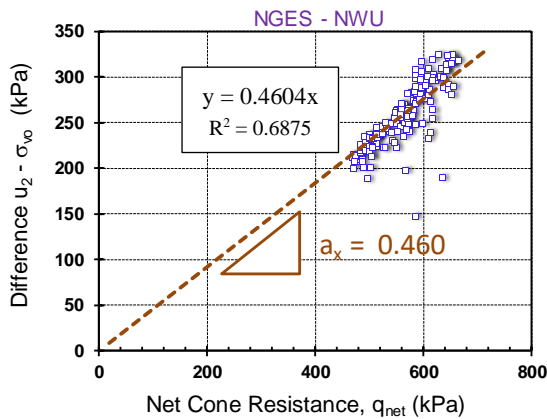


Figure 8. Evaluation of slope parameter ( $a_x$ ) for the  $I_R$  solution as a function of  $(u_2 - \sigma_{v0})$  vs.  $q_{net}$  using CPTu data in soft Chicago clay at Northwestern University, IL

In Figure 9, the net cone tip resistance ( $q_{net}$ ) is plotted versus the effective cone tip resistance ( $q_E$ ), giving a slope value of  $a_y = 1.846$ . This slope value is used with the friction angle of 28.8 degrees in Eq. (15) to give an undrained rigidity index  $I_R = 142.9$ .

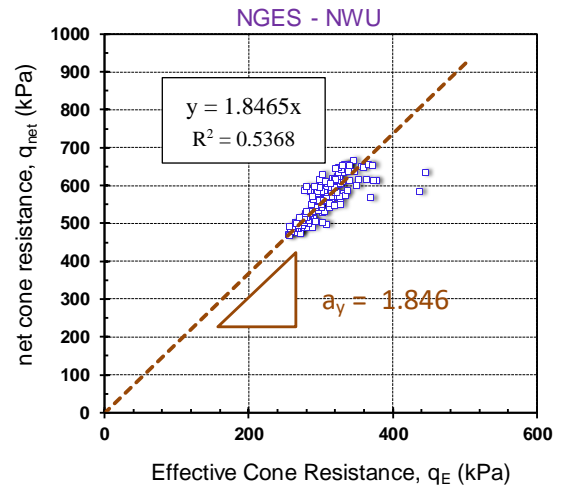


Figure 9. Evaluation of slope parameter ( $a_y$ ) for the  $I_R$  solution in terms of  $q_{net}$  vs.  $q_E$  using CPTu data in soft Chicago clay

Finally, Figure 10 shows the evaluation of the slope parameter ( $a_z$ ) where  $(u_2 - \sigma_{v0})$  is plotted versus effective cone tip resistance ( $q_E$ ), giving a slope value of  $a_z = 0.846$  together with the NTH evaluated friction angle in Eq. (16) to obtain a value of rigidity index  $I_R = 142.9$ .

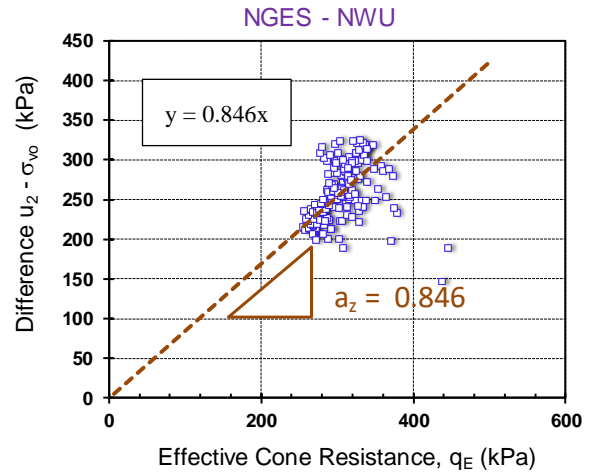


Figure 10. Evaluation of slope parameter ( $a_z$ ) for the  $I_R$  solution as a function of  $(u_2 - \sigma_{v0})$  vs.  $q_E$  using CPTu data in soft Chicago clay

By comparing the obtained rigidity index values using the three slopes, it can be seen that all three solutions give similar values for  $I_R \approx 143$ . The obtained  $I_R$  value is used to obtain the cone bearing factor ( $N_{kt}$ ) as per Eq. (20) for evaluating the undrained shear strength ( $s_u$ ). Using  $I_R = 143$  the corresponding  $N_{kt} = 10.52$  which provides very good agreement with reference CAUC triaxial data for this site, reported by Finno and Chung [23], as evident by Figure 11.

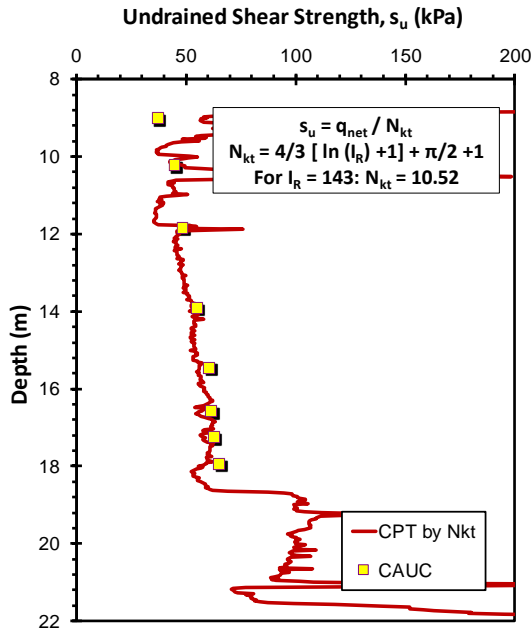


Figure 11. Undrained shear strength profile for soft Chicago clay using  $I_R$  and cone bearing factor  $N_{kt}$  (Lab data from [23])

Applying the three OCR equations from the hybrid SCE-CSSM solution to the results of piezocone sounding from Figure 4 with  $I_R = 143$  and  $\phi' = 28.3^\circ$  within the Deerfield and Blodgett soft clay layers, the individual profiles are seen to be consistent, as evidenced in Figures 12 and 13. When compared with laboratory-measured  $\sigma_p'$  and OCR profiles reported by Chung and Finnø [22], the CPTu soundings give a very good match.

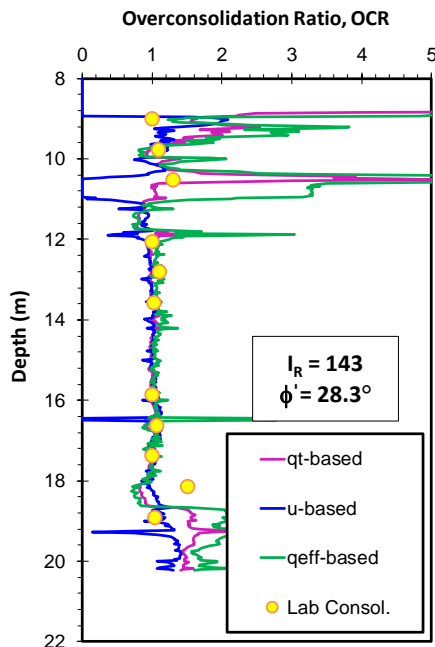


Figure 12. Profiles of OCR from CPTu using SCE-CSSM solutions in soft Chicago clay

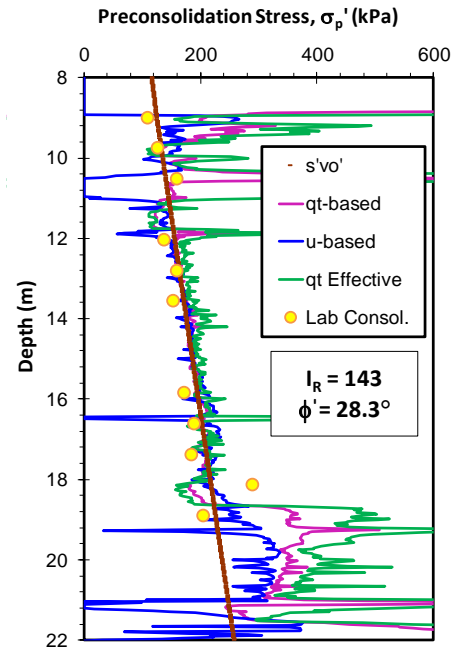


Figure 13. Profiles preconsolidation stress from CPTu using SCE-CSSM solutions in soft Chicago clay

Figure 14 presents a design chart with contour lines for different effective friction angles ( $\phi'$ ), relating the slope parameter ( $a_q$ ) with the evaluated rigidity index value ( $I_R$ ). From the piezocone sounding, the slope  $a_q$  is determined as a single value for any clay deposit by taking the slope of a plot of the parameter ( $U^* - 1$ ) versus  $Q$ , or alternatively as the slope of  $(u_2 - \sigma_{vo})$  versus  $(q_t - \sigma_{vo})$ . The effective friction angle can be determined either from laboratory measurements or evaluated from a method like NTH. By knowing the slope value and the effective friction angle, one can evaluate an operational value for the rigidity index.

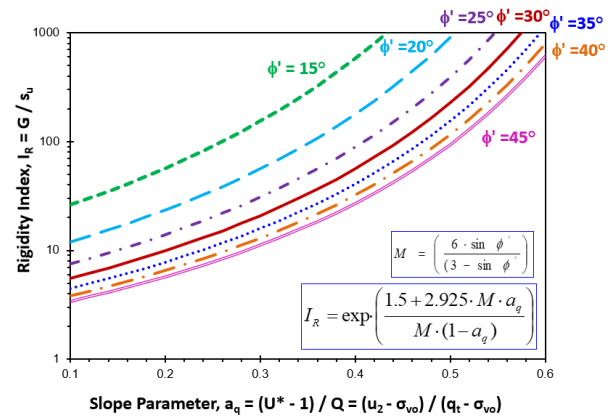


Figure 14. Contour lines for different effective friction angles ( $\phi'$ ) for rigidity index ( $I_R$ ) evaluation from the slope parameter ( $a_q$ )

## 7. Conclusions

Using a hybrid spherical cavity expansion – critical state framework, it is shown that the operational value of rigidity index ( $I_R$ ), overconsolidation ratio (OCR), and undrained shear strength ( $s_u$ ) are all obtained from the cone tip resistance and porewater pressure readings, expressed in terms of their normalized quantities. For the

evaluation of rigidity index, three expressions are provided that rely on different slopes;  $a_x$ ,  $a_y$  and  $a_z$ .

A detailed case study of soft Chicago clay at the National Geotechnical Experimentation Site (NGES) at Northwestern University is presented to demonstrate the effectiveness of the methodology and the resemblance in the obtained operational rigidity index value regardless of the used cone readings and its corresponding slope. The assessed  $I_R$  value is used to evaluate profiles of undrained shear strength and overconsolidation ratio (OCR). The effective stress friction angle ( $\phi'$ ) is assessed using an available limit plasticity solution from NTH [18] that compares well with CAUC triaxial tests.

## 8. Acknowledgments

The authors sincerely appreciate the financial support provided by the ConeTec Group of Vancouver, BC.

## 9. References

- [1] Vardanega, P.J. and Bolton, M.D. (2013). The stiffness of clays and silts: normalizing shear modulus and shear strain. *Journal of Geotechnical & Geoenvironmental Engineering*, doi:10.1061/(ASCE)GT.1943.5606.0000887.
- [2] Krage, C.P., Broussard, N.S., & DeJong, J.T. (2014). Estimating rigidity index ( $I_R$ ) based on CPT measurements. *Proceedings of the 3<sup>rd</sup> International Symposium on Cone Penetration Testing*, Las Vegas: 727-735. [www.usucger.org](http://www.usucger.org)
- [3] Mayne, P.W. (2005). *Integrated ground behavior: in-situ and lab tests. Deformation Characteristics of Geomaterials*, Vol. 2 (Proc. IS Lyon'03), Taylor & Francis, London: 155-177.
- [4] Mayne, P.W. (2007). *In-situ test calibrations for evaluating soil parameters, Characterization & Engineering Properties of Natural Soils*, Vol. 3, Taylor & Francis, London: 1602-1652.
- [5] Mayne, P.W. (2001). Stress-strain-strength-flow parameters from enhanced in-situ tests. *Proceedings International Conference on In-Situ Measurement of Soil Properties & Case Histories (In-Situ 2000)*, Bali, Indonesia, 47-69.
- [6] Vesić, A.S. (1977). *Design of Pile Foundations. Synthesis of Highway Practice 42*. Transportation Research Board, National Research Council, Washington, DC: 68 p.
- [7] Keaveny, J. (1985). *In-situ determination of drained and undrained soil strength using the cone penetration test*, Ph.D. Dissertation, University of California, Berkeley, 371p.
- [8] Schnaid, F., Sills, G.C., Soares, J.M., & Nyirenda, Z. (1997). Predictions of the coefficient of consolidation from piezocone tests. *Canadian Geotechnical J.* 34 (2): 315-327.
- [9] Konrad, J.M. and Law, K. (1987). Undrained shear strength from piezocone. *Canadian Geotechnical J.* 24: 392-405.
- [10] Teh, C.I. & Housley, G.T. (1991). An analytical study of the cone penetration test in clay. *Geotechnique* 41 (1): 17-31.
- [11] Yu, H. S. & Mitchell, J. K. (1998). Analysis of cone resistance: review of methods. *Journal of Geotechnical and Geoenvironmental Engineering*, 124(2), 140-149.
- [12] Keaveny, J. and Mitchell, J.K. (1986). Strength of fine-grained soils using the piezocone. *Use of In-Situ Tests in Geotechnical Engrg. (GSP 6)*, ASCE, Reston/VA, 668-685.
- [13] Kulhawy, F.H. and Mayne, P.W. (1990). *Manual on Estimating Soil Properties for Foundation Design*, Report No. EL-6800, Electric Power Research Institute, Palo Alto, CA, August 1990, 306 pages. Download from: [www.epri.com](http://www.epri.com)
- [14] Ladd, C.C. (1991). Stability evaluation during staged construction. (The 22<sup>nd</sup> Terzaghi Lecture), *Journal of Geotechnical Engineering* 117 (4): 540-615.
- [15] Mayne, P.W. (2016). Evaluating effective stress parameters and undrained shear strengths of soft-firm clays from CPT and DMT. *In Pursuit of Best Practices - Proc. 5<sup>th</sup> Intl. Conf. on Geotechnical & Geophysical Site Characterization (ISC-5, Gold Coast)*, Australian Geomechanics Society, Vol. 1: 19-40
- [16] Mayne, P.W. (1991). Determination of OCR in clays by piezocone tests using cavity expansion and critical state concepts. *Soils and Foundations* 31 (2): 65-76.
- [17] Chen, B.Y. and Mayne, P.W. (1994). *Profiling the Overconsolidation Ratio of Clays by Piezocone Tests*, Report No. GIT-CEE/GEO-94-1 submitted to National Science Foundation by Georgia Institute of Technology, Atlanta, 280 p.
- [18] Senneset, K., Sandven, R., Janbu, N. (1989). Evaluation of soil parameters from piezocone tests. *Transportation Research Record 1235*, National Academies Press, Washington DC: 24-37.
- [19] Mayne, P.W. (2007). *NCHRP Synthesis 368 on Cone Penetration Test*. Transportation Research Board, National Academies Press, Washington, D.C., 118 pages.
- [20] Finno, R.J., Gassman, S.L., and Calvello, M. (2000). *The NGES at Northwestern University. National Geotechnical Experimentation Sites (GSP 93)*, ASCE, Reston, VA: 130 - 159.
- [21] McGillivray, A. V. (2007). *Enhanced integration of shear wave velocity profiling in direct push site characterization systems*. Ph.D. Dissertation. Civil & Environmental Engineering, Georgia Institute of Technology, 393p.
- [22] Chung, C.K., and Finno, R.J. (1992). Influence of depositional processes on the geotechnical parameters of Chicago glacial clays. *Engineering Geology*, 32(4), 225-242.
- [23] Finno, R.J. and Chung, C.K. (1992). Stress-strain strength responses of compressible Chicago glacial clays, *Journal of Geotechnical Engineering*, ASCE, Vol. 119, No. 10, 1607-1625.